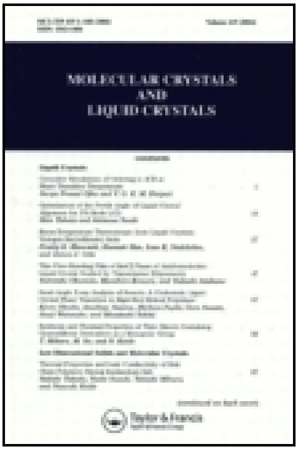

Molecular Crystals and Liquid Crystals
Publication details, including instructions for authors and subscription information:
http://www.tandfonline.com/loi/gmcl20

Synthesis, Structure, And Physical Properties Of An Electron Acceptor: Trifluoromethyl-TCNQ (CF 3 TCNQ)

Hideo Ikegami [a] , Chin-Hong Chong [a] , Hideki Yamochi [a] & Gunzi Saito [a]
[a] Division of Chemistry, Graduate School of Science, Kyoto University, Kyoto, Japan

To cite this article: Hideo Ikegami, Chin-Hong Chong, Hideki Yamochi & Gunzi Saito (2002): Synthesis, Structure, And Physical Properties Of An Electron Acceptor: Trifluoromethyl-TCNQ (CF 3 TCNQ), Molecular Crystals and Liquid Crystals, 382:1, 21-35

To link to this article: http://dx.doi.org/10.1080/713738752

Mol. Cryst. Liq. Cryst., Vol. 382, pp. 21–35
Copyright © 2002 Taylor & Francis
1058-725X/02 \$12.00 + .00
DOI: 10.1080/10587250290120242

SYNTHESIS, STRUCTURE, AND PHYSICAL PROPERTIES OF AN ELECTRON ACCEPTOR: TRIFLUOROMETHYL-TCNQ (CF_3TCNQ)

Hideo Ikegami, Chin-Hong Chong, Hideki Yamochi, and Gunzi Saito
Division of Chemistry, Graduate School of Science,
Kyoto University, Kyoto, Japan

An electron acceptor molecule of tetracyanoquinodimethane (TCNQ) derivative; trifluoromethyl-TCNQ (CF_3TCNQ) was synthesized and its crystal structure was determined. CF_3TCNQ was found to be a strong electron acceptor comparable to 2,5-difluoro-TCNQ. The adiabatic electron affinity and molecular on-site Coulomb energy of CF_3TCNQ were estimated to be 2.96–3.05 eV and 4.74 eV, respectively. The acidity of dihydro-CF_3TCNQ in N,N-dimethylformamide/H_2O was estimated to be $pK_1 = 5.30$ and $pK_2 = 8.20$. The molecular and crystal structures and molecular orbitals of CF_3TCNQ are described.

Keywords: trifluoromethyl-TCNQ; electron acceptor; preparation; structure; molecular orbital; acidity

INTRODUCTION

Tetracyanoquinodimethane (TCNQ) and its derivatives have received unabated interest as electron acceptor molecules in the field of organic conductors of the charge transfer (CT) type. These include organic metals

Received 26 February 2001; accepted 22 March 2001.

This work was in part supported by a Grant-in-Aid for Scientific Research from the Ministry of Education, Science, Sports, and Culture, Japan, a Grant from CREST (Core Research for Evolutional Science and Technology) of Japan Science and Technology Corporation (JST), a fund from "Research for Future" from Japan Society for Promotion of Science, and a fund from the International Joint Research Grant Program of the New Energy and Industrial Technology Development Organization (NEDO).

Address correspondence to Gunzi Saito, Division of Chemistry, Graduate School of Science, Kyoto University, Sakyo-ku, Kyoto 606-8502, Japan. E-mail: saito@kuchem.kyoto-u.ac.jp

(e.g. TTF·TCNQ)[1]*, metallic Langmuir-Blodgett films (BEDO-TTF(BO)·decyl-TCNQ, BO·$(MeO)_2$TCNQ) [2], neutral-ionic phase transition system (3,3′,5,5′-tetramethylbenzidine·TCNQ) [3], organic semiconductor condenser (N-alkyl-isoquinolinium·TCNQ) [4], switching and memory system (Cu·TCNQ [5a], $TTeC_1$-TTF·TCNQ [5b]), nonlinear optical materials (perylene·TCNQ [6], zwitterionic one [7]), and molecular rectifiers [8].

For tuning both the Fermi level and density of states in a metal, it is crucial to obtain a variety of TCNQ derivatives which vary little in size and cover a wide range of electron-accepting ability. Also of importance is how the asymmetry of the component molecule affects the electrical and magnetic properties of the CT complexes. In order to search for highly conducting Langmuir-Blodgett films of CT type it is of interest to use a TCNQ derivative having a short side chain. With these properties in mind we report here the synthesis, structure and physical properties of a TCNQ derivative, trifluoromethyl-TCNQ (CF_3TCNQ).

The main molecules in this paper are presented in Scheme 1.

EXPERIMENTAL

Measurement

The melting points were not corrected. Cyclic voltammetric measurements were performed in 0.1 M solutions of tetrabutylammonium tetrafluoroborate (TBA·BF_4) in acetonitrile (MeCN) with Pt electrodes vs. saturated calomel electrode (SCE) or Ag/AgCl at 10–100 mV sec^{-1} and 20–22°C. The optical measurements were carried out on a Perkin-Elmer 1600 Series FT-IR (resolution 4 cm^{-1}) for the IR and near-IR (NIR) regions (400–7800 cm^{-1}) in KBr and on a SHIMADZU UV-3100 spectrometer for the UV-VIS-NIR region (3800–42000 cm^{-1}) in KBr or in solution. The mass spectra (MS) were measured by the EI method on a Jeol AMII spectrometer. The instrument used for pH measurements was a Toa HM-5ES glass electrode. The pH meter was corrected using tetraborate ($pH = 9.18$ at 25°C), phosphate ($pH = 6.86$ at 25°C), and phthalate ($pH = 4.01$ at 25°C) standard solutions. The subsequent titrations were carried out with the addition of standard sodium hydroxide solution (0.1 M). All titrations were run at 22 ± 1°C, and the ion strengths fixed to a constant value (0.1 M) using sodium tetrafluoroborate. The intensity data of the structural analysis were collected on an automatic four circle diffractometer with a

---

*Chemicals in text: TCNQ, tetracyanoquinodimethane; TTF, tetrathiafulvalene; TMTTF, tetramethyl-TTF; BEDO-TTF, bisethylenedioxy-TTF; $TTeC_1$-TTF, tetrakismethyltelluro-TTF; EOET-TTF, ethylenedithioethylenedioxy-TTF; BEDT-TTF, bisethylenedithio-TTF; BEDO-DBTTF, bisethylenedioxy-dibenzoTTF; HMTTeF, hexamethylenetetratellurafulvalene.

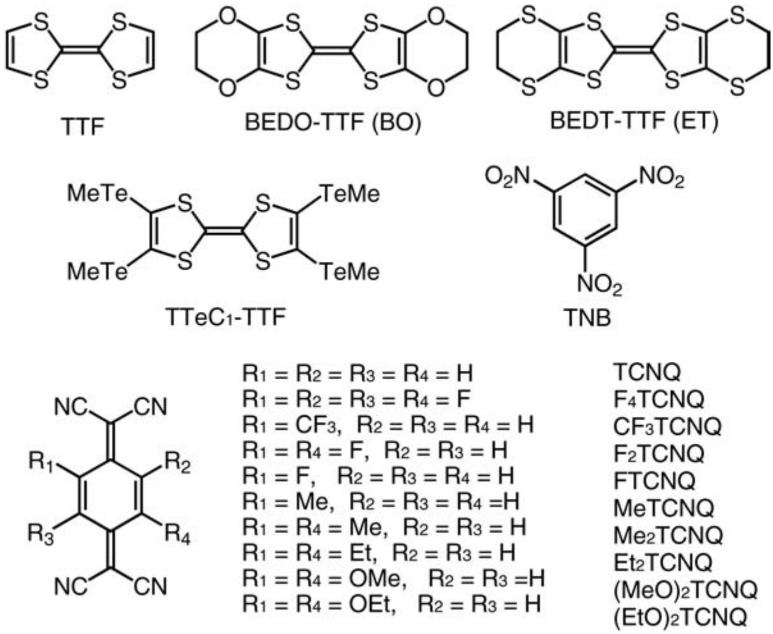

SCHEME 1 Chemical structures of compounds discussed in the text.

monochromated MoK_α radiation at room temperature. The structures were determined by direct methods. The refinements of the structures were performed by full matrix least squares method. The semiempirical molecular orbital calculations were performed using MOPAC 97 with the AM1 parameterization.

Synthesis

The synthetic procedure of CF_3TCNQ is depicted in Figure 1. The diiodo derivative (**2**) of 1,4-dibromo-2-trifluoromethylbenzene (**1**) was prepared using the method of Suzuki et al. [9]. A mixture of **1** (25.0 g, 82.9 mmol), KI (46.5 g, 280 mmol), and CuI (16.1 g, 84.4 mmol) in 50 mL of hexamethylphosphoramide was heated to 145°C and stirred under nitrogen for 19 h and then cooled to room temperature. After adding 360 mL of 1 N HCl, the reaction mixture was extracted with diethylether (ca. 100 mL × 4). The organic layer was concentrated to ca. 20 mL then cooled in ice to precipitate 1,4-diiodo-2-trifluoromethylbenzene (**2**), which was collected on a glass filter and dried (white powder, 28.8 g, 72.4 mmol yield 88.2%, m.p. 100.9–101.6°C).

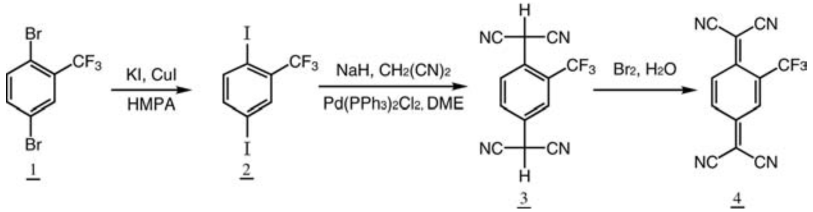

FIGURE 1 Synthetic scheme of CF_3TCNQ.

2 was converted to 2-trifluoromethyl-1,4-benzenedimalononitrile (CF_3-H_2TCNQ, **3**) using the method of Uno et al. [10] and oxidized to CF_3TCNQ (**4**) by adding bromine/water [11]. A mixture of NaH (40% oil 16.9 g, 423 mmol), malononitrile (19.0 g, 287 mmol), bis(triphenylphosphonium)$PdCl_2$ [$Pd(PPh_3)_2Cl_2$] (2.01 g, 2.87 mmol) and **2** (28.6 g, 72.0 mmol) in 320 mL of dry 1,2-dimethoxyethane was refluxed for 17.7 h under nitrogen and cooled to room temperature. After adding 240 mL of 1 N HCl, the supernatant fluid was discarded by decantation. The brown oily product (**3**) was washed with water a few times and suspended by stirring it in 80 mL of water containing 4 mL of bromine (76.9 mmol). The yellowish brown solid of CF_3TCNQ (**4**) was collected on a glass filter. The crude product was dried under vacuum and recrystallized from 1080 mL of benzene/diethylether (5:1) twice to yield a yellowish orange powder (5.33 g, yield 24.2%), which was further purified by a conventional sublimation then by a gradient sublimation (0.25 Torr, 170°C) to yield orange granules (**4**) (2.42 g, yield 11.0%, m.p. 185.0–185.2°C; MS (70 eV) m/e 272 (M^+, 100), 273 (M^++1, 17.4); ^{1}H NMR($CDCl_3$) δ 7.94 (1H, s), 7.82 (1H, d), 7.61 (1H, d); IR(KBr) 2223 cm^{-1} ($C\equiv N$); UV-VIS (MeCN) 375 nm (sh, ε 3.6×10^3), 394 nm (ε 5.42×10^3). Anal. Calcd for $C_{13}H_3N_4F_3$; C, 57.37; H, 1.11; N, 20.58; F, 20.94; Found C, 57.51; H, 1.40; N, 20.88; F, 21.04%. The pK_a values were measured on purified CF_3-H_2TCNQ.

ELECTRON-ACCEPTING ABILITY AND ON-SITE COULOMB REPULSIVE ENERGY OF CF_3TCNQ

Redox Potential

The cyclic voltammogram displays two reversible one-electron redox waves. Table 1 summarizes the first ($E^1_{1/2}$ for the process of $A+e^- \rightleftarrows A^{1-\bullet}$) and second ($E^2_{1/2}$ for $A^{1-\bullet}+e^- \rightleftarrows A^{2-}$) redox potentials (vs. SCE, MeCN) and the difference between them (ΔE) for several related TCNQs. The $E^1_{1/2}$ value of CF_3TCNQ is a little higher than that of F_2TCNQ, suggesting that CF_3TCNQ is a considerably strong electron acceptor. As shown in

TABLE 1 Redox Potentials, Charge Transfer Transition Energies, and Hammett σ Values of some TCNQ Derivatives

TCNQs	Cyclic voltammetry (V)[a] $E^1_{1/2}$	$E^2_{1/2}$	ΔE	$h\nu_{CT}$[b] pyrene ($\times 10^3$ cm^{-1})	Hammett σ[c]
F_4TCNQ	0.60	0.05	0.55	10.5	0.80
CF_3TCNQ	0.44	−0.14	0.58	11.6	0.49
F_2TCNQ	0.41	−0.13	0.54	11.6	0.40
FTCNQ	0.32	−0.24	0.56	12.3	0.20
TCNQ	0.22	−0.34	0.56	12.8	0
MeTCNQ	0.19	−0.33	0.52	13.4	−0.12
Me_2TCNQ	0.15	−0.34	0.49	13.7	−0.24
Et_2TCNQ	0.15	−0.34	0.49	13.9	−0.22
$(MeO)_2$TCNQ	0.05	−0.44	0.49	14.7	−0.54
$(EtO)_2$TCNQ	0.01	−0.46	0.47	15.3	−0.48

[a] $E^1_{1/2}$ and $E^2_{1/2}$ are the average values of the reduction and oxidation peak-potentials for the processes $A^0 \rightleftarrows A^{-\bullet}$ and $A^{-\bullet} \rightleftarrows A^{2-}$, respectively, Pt electrodes, CH_3CN, 0.1 M TBA•BF_4, 20–22°C, 10–20 mV s^{-1}. $E^1_{1/2}$ and $E^2_{1/2}$ of CF_3TCNQ vs. Ag/AgCl are 0.37 and −0.14 V, respectively.

[b] Pyrene CT complex in $CHCl_3$ solution at room temperature. Hexamethylbenzene and anthracene CT complexes of CF_3TCNQ exhibit CT bands at 15.3 and 11.2×10^3 cm^{-1}, respectively.

[c] See all references listed in [13].

Figure 2, the first (or second) redox potential of CF_3TCNQ in MeCN is on the linear line between the $E^1_{1/2}$ (or $E^2_{1/2}$) and Hammett σ values [12], giving the following equations (γ: correlation coefficient):

$$E^1_{1/2} = 0.424\sigma + 0.242 \ (\gamma = 0.995), \tag{1}$$

$$E^2_{1/2} = 0.353\sigma - 0.281 \ (\gamma = 0.977). \tag{2}$$

The estimation of electron affinity (E_A) based on the redox potentials is usually done by using an empirical relation between the experimentally observed E_As and redox potentials [13]. Taking into account the large ambiguity caused by both the lack of adequate numbers of experimentally determined E_A values and the significant difference of the magnitude of solvation energy included in the redox potentials from system to system [14], the adiabatic E_A value of CF_3TCNQ is estimated as 2.96 ± 0.10 eV using the empirical relation. Equation (3), as proposed in Saito et al. [15]:

$$E_A = 0.858\ E^1_{1/2}\ (\text{vs. SCE in MeCN}) + 2.59. \tag{3}$$

The second redox potentials of TCNQs in Table 1 correlate linearly with the first ones with the slope less than unity as expressed by Equation (4):

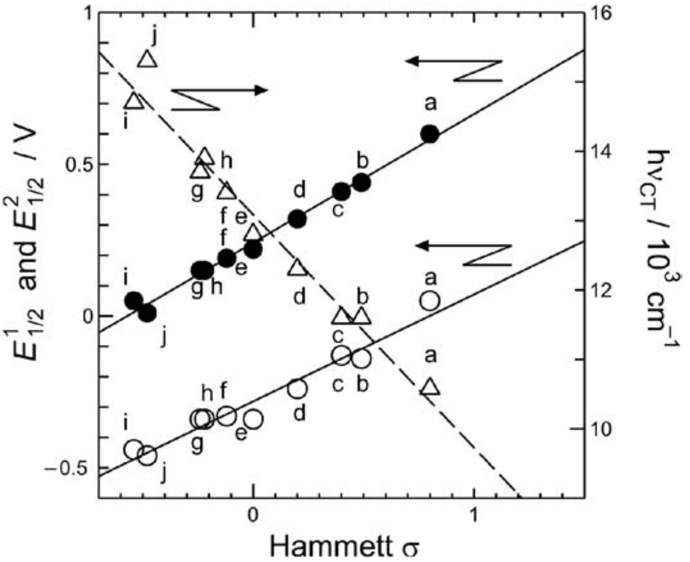

FIGURE 2 Plots of half-wave redox potentials ($E^1_{1/2}$ (closed circle) and $E^2_{1/2}$ (open circle) vs. SCE) of TCNQs and charge transfer transition energies (triangle) of complexes of TCNQs with pyrene ($h\nu_{CT}$(pyrene·A)) against the Hammett σ values [12]. Solid and dashed lines are the results of least squares fit. The letters indicate TCNQ derivatives RTCNQ (R = F_4(a), CF_3(b), F_2(c), F(d), H(e), Me(f), Me_2(g), Et_2(h), $(MeO)_2$(i), $(EtO)_2$(j)).

$$E^2_{1/2} = 0.834\,E^1_{1/2} - 0.479 \tag{4}$$

The difference of the first and second redox potentials, ΔE ($= E^1_{1/2} - E^2_{1/2}$), decreases with the decreasing acceptor ability of the TCNQs as seen in Table 1. From the linearity, the molecular on-site Coulomb energy U_0 is evaluated as 4.74 eV using an empirical equation:

$$U_0(\text{TCNQs}) = 0.17E^1_{1/2}\ (\text{vs. SCE in MeCN}) + 4.67, \tag{5}$$

which is derived from a similar procedure to that described in Akutagawa and Saito [16a]. The estimated U_0 value of CF_3TCNQ is not much different from those of TCNQ and F_4TCNQ, calculated using the redox potential data in MeCN ($U_0 = 4.70–4.77$ eV) [16a].

Charge Transfer Absorption

The electron-accepting ability of an acceptor molecule is appropriately estimated by the CT absorption energy of a weak CT complex in an inert solvent. The CF_3TCNQ molecule gave CT absorption energies ($h\nu_{CT}$) not much different from those of the F_2TCNQ molecule. A plot of the $h\nu_{CT}$($D{\cdot}CF_3TCNQ$, D = pyrene, hexamethylbenzene, anthracene) values in Table 1 against the $h\nu_{CT}$(D·TNB, TNB = *s*-trinitrobenzene) values gave a straight line, as has been observed for the case of TCNQ, *p*-chloranil, and C_{60} molecules [15]. By the same procedure as described in Saito et al. [15] the difference of the CT absorption energies ($\Delta h\nu_{CT} - h\nu_{CT}(D{\cdot}TNB) - h\nu_{CT}$ ($D{\cdot}CF_3TCNQ$)) was found to be $10.5 \times 10^3\,cm^{-1}$. An empirical relation: Equation 6 [15] is utilized to give the $E_A = 3.05 \pm 0.10\,eV$ of CF_3TCNQ, which is in good agreement with that estimated from the redox potential. As shown in Figure 2, the $h\nu_{CT}$(pyrene·A) values in Table 1 are linearly related to the Hammett σ values:

$$E_A\ (\text{in eV}) = 0.108\,\Delta h\nu_{CT}(\text{TNB vs. A in } 10^3\,\text{cm}^{-1}) + 1.92, \qquad (6)$$

PROTON-DONATING ABILITY (ACIDITY) OF CF_3-H_2TCNQ

The dissociation constants of dihydro-CF_3TCNQ (CF_3-H_2TCNQ) for the processes expressed by Equations (7) and (8) were measured to be $pK_1 = 5.30$ and $pK_2 = 8.20$ in a mixed solution of DMF/H_2O (7/3):

$$CF_3{-}H_2TCNQ \overset{K_1}{\rightleftarrows} CF_3{-}HTCNQ^{1-} + H^+, \qquad (7)$$

$$CF_3\text{-}HTCNQ^{1-} \overset{K_2}{\rightleftarrows} CF_3TCNQ^{2-} + H^+. \qquad (8)$$

These values are between those of F_4TCNQ ($pK_1 = 4.01$, $pK_2 = 7.20$) and TCNQ (7.10, 10.30) [16a]. Fairly good relations both between the pK and Hammett σ values ($pK_1 = 6.99{-}3.16\sigma$, $pK_2 = 10.10{-}3.17\sigma$) and between the pK_1 and pK_2 values ($pK_2 = pK_1{+}3.11$) are found to exist using the data of Me_2TCNQ (7.60, 11.30) [16a].

MOLECULAR AND CRYSTAL STRUCTURES AND MOLECULAR ORBITAL CALCULATION OF CF_3TCNQ

Orange granules of CF_3TCNQ crystallize in the triclinic, $P\bar{1}$. Two crystallographically independent CF_3TCNQ molecules were found, and their molecular and crystal structures are presented in Figure 3. The lattice and the atomic parameters are summarized in Tables 2 and 3, and some bond lengths and angles are presented in Table 4.

The CF_3 group is ordered at room temperature. The carbon atom of the CF_3 group is not on the nearly planar TCNQ plane but deviates by 0.46 Å and 0.25 Å for CF_3TCNQ molecules I and II, respectively. As seen from the bond angles, the dicyanomethylene group remote from the CF_3 group is sterically relaxed. On the other hand, the steric hindrance between

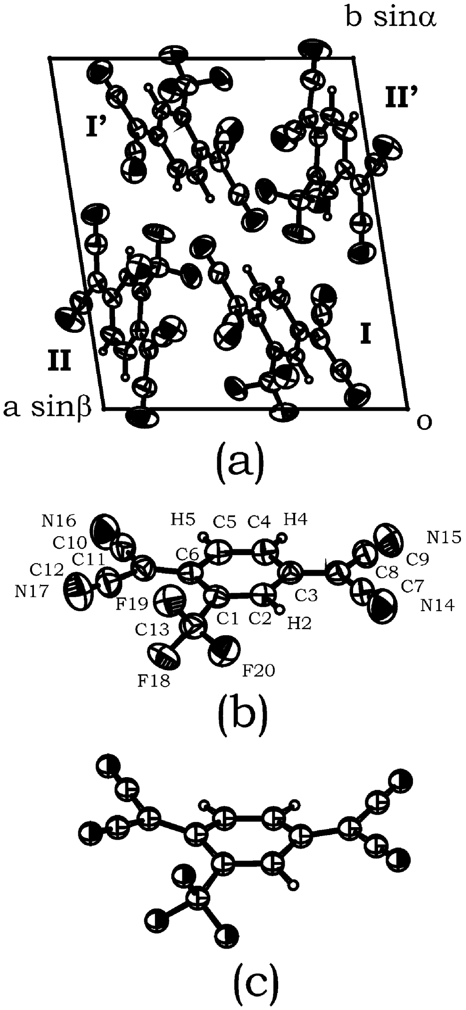

FIGURE 3 (a) ORTEP drawing of the crystal structure of CF_3TCNQ projected along the c-axis. The symmetry operations for I and II are (x,y,z), and for I′ and II′ are (1−x,1−y,1−z). (b) The atomic numbering scheme of the CF_3TCNQ(I), to which we add 20 to obtain the atomic numbers for CF_3TCNQ(II). (c) The molecular shape obtained from the geometry optimization of CF_3TCNQ by a semiempirical molecular orbital calculation.

TABLE 2 Crystal Data, Data Collection, and Reduction Parameters of CF_3TCNQ

	Neutral CF_3TCNQ
Formula	$C_{13}H_3N_4F_3$
Formula wt	272.18
Crystal dimension	$0.18 \times 0.43 \times 0.48\,mm^3$
Crystal system	triclinic
Space group	$P\,\bar{1}$
a/Å	11.412(4)
b/Å	13.323(4)
c/Å	8.075(4)
α/deg	87.86(3)
β/deg	86.93(3)
γ/deg	81.13(3)
V/$Å^3$	1210.7(3)
Z	4
D_{calc}, g/cm^3	1.49
Diffractometer	MAC SCIENCE MXC^{χ}
Radiation	MoKα
Scan mode	$2\theta-\omega$
$2\theta_{max}$	55°
No. of intensity meas	4462
Criterion for obsd. reflection	$F_0 > 6\sigma(F_0)$
Reflections used in L.S.	3095
No. of refined parameters	433
R	0.0717

Refinement conditions: Anisotropic temperature factors were adopted to the nonhydrogen atoms. The positional parameters of hydrogen atoms were calculated assuming the sp^2 configuration of carbon atoms bonding to it, isotropic temperature factor of $U = 0.05\ Å^2$, and C-H bond length of 1.00 Å.

dicyanomethylene and the adjacent CF_3 groups is obvious from the distorted bond angles; namely, α_2 (122.8° and 122.4°), β_2 (127.3°, 127.6°), and γ_2 (128.2°, 128.9°) are widened while α_1(116.7°, 117.2°) and β_1 (117.5°, 116.4°) are narrowed, and furthermore the angle of C_{11}-C_{12}-N_{17} (see Figure 3b, 174.0°) is less than the other corresponding C-C-N angles (177.2, 177.2, and 179.6°) (Table 4).

It has been known for TCNQ derivatives that the molecular length is elongated along the long molecular axis but shortened along the short molecular axis as the electron acceptor strength increases [17]. This tendency is also noted in CF_3TCNQ molecules.

The permanent dipole moments of CF_3TCNQ molecules, which were estimated to be 1.87–1.93 Debye by MOPAC calculation, were cancelled

TABLE 3 Atomic Coordinates and Equivalent Isotropic Parameters of CF_3TCNQ Molecules

Atom	x	y	z	Beq (Å^2)
C1	0.40670	0.16510	0.37610	3.339870
C2	0.34170	0.14890	0.51570	3.479370
C3	0.31680	0.22190	0.64630	3.482000
C4	0.36500	0.31460	0.62130	3.882040
C5	0.42590	0.33300	0.47960	3.832040
C6	0.44930	0.26230	0.34460	3.358300
C7	0.20040	0.10960	0.80750	4.516330
C8	0.25270	0.20050	0.78750	3.726760
C9	0.23440	0.26870	0.92300	4.384740
C10	0.55280	0.38840	0.19850	4.537390
C11	0.50680	0.29320	0.20400	3.945210
C12	0.53240	0.24100	0.05010	5.082190
C13	0.43780	0.07620	0.26050	4.400530
N14	0.15840	0.03780	0.82380	6.932410
N15	0.21890	0.31930	1.03410	6.158630
N16	0.59240	0.46180	0.18930	6.835030
N17	0.55580	0.20740	−0.07660	7.064010
F18	0.55470	0.05850	0.22500	5.626990
F19	0.38370	0.09190	0.11810	5.700680
F20	0.40870	−0.00950	0.33010	5.821750
H2	0.30980	0.08320	0.52880	
H4	0.35510	0.36640	0.70940	
H5	0.45690	0.39970	0.47010	
C21	0.81790	0.33420	−0.15330	3.139850
C22	0.85180	0.37640	−0.01810	3.263550
C23	0.91650	0.31650	0.10980	3.584640
C24	0.93450	0.20860	0.09820	4.192610
C25	0.90040	0.16630	−0.03630	4.053120
C26	0.84400	0.22470	−0.17320	3.318820
C27	0.94210	0.46990	0.25730	4.447900
C28	0.95760	0.36190	0.24190	3.882040
C29	1.02090	0.30310	0.36960	4.753200
C30	0.85570	0.06200	−0.30850	5.200620
C31	0.82260	0.17000	−0.30880	3.795190
C32	0.77040	0.20660	−0.46070	4.674250
C33	0.75040	0.40440	−0.27770	4.174190
N34	0.92930	0.55530	0.26730	6.666590
N35	1.06710	0.25430	0.47380	6.650800
N36	0.87800	−0.02360	−0.31000	8.298360
N37	0.73210	0.22890	−0.58740	6.479720
F38	0.64550	0.37890	−0.30540	5.548030
F39	0.81120	0.40640	−0.42370	5.621730
F40	0.73020	0.50040	−0.22760	6.563950
H22	0.83400	0.45150	−0.00380	
H24	0.97340	0.16460	0.18920	
H25	0.91380	0.09070	−0.04540	

Beq $= (4/3)\ \Sigma\ B_{ii}^2$. For the atomic numbering, see Figure 3b.

TABLE 4 Bond Lengths, Angles, and Dimension of CF_3TCNQ Molecules. Comparison of CF_3TCNQ Intramolecular Geometry

Distance (Å)	CF_3TCNQ (I)	CF_3TCNQ (II)	Angle (°)	CF_3TCNQ (I)	CF_3TCNQ (II)
a1	1.341(6)	1.344(8)	$\alpha1$	116.7(4)	117.2(5)
a2	1.345(7)	1.348(8)	$\alpha2$	122.8(4)	122.4(5)
b1	1.454(7)	1.449(8)	$\beta1$	117.5(5)	116.4(5)
b2	1.461(7)	1.456(8)	$\beta2$	127.3(5)	127.6(5)
b3	1.431(7)	1.426(8)	$\gamma1$	120.2(5)	120.3(5)
b4	1.448(7)	1.445(8)	$\gamma2$	128.2(5)	128.9(5)
c1	1.363(8)	1.390(8)	$\delta1$	111.6(5)	110.9(5)
c2	1.366(7)	1.383(8)	$\delta2$	116.8(5)	116.0(5)
d1	8.168(7)	8.006(7)			
d2	8.771(7)	8.862(7)			
e1	4.165(7)	4.149(7)			
e2	4.339(7)	4.379(7)			

The notation of each interatomic distance and bond angle is as follows:

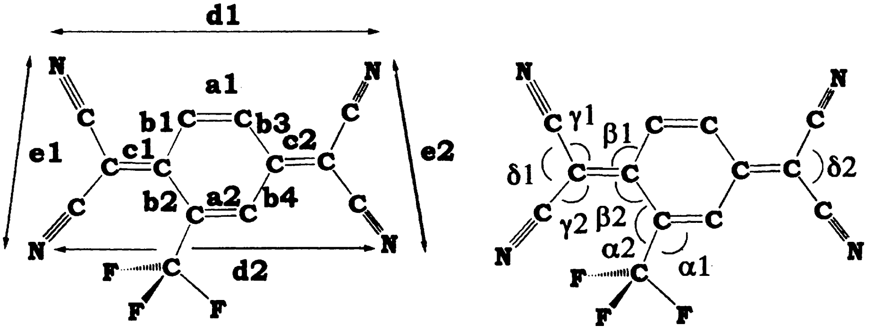

out by the presence of the inversion center at the center of the unit cell in the crystal, as shown in Figure 3a.

To understand the effect of the CF_3 group on the acceptor strength of CF_3TCNQ, molecular orbital calculations were performed. Table 5 summarizes the orbital energies and the atomic orbital (AO) coefficients of the LUMOs for the molecular geometry, determined by the crystal structure analysis, along with those for the optimized geometry of CF_3TCNQ. Although the optimized configuration shows the concave shape along the molecular long axis (Figure 3c), the absolute values of the AO coefficients obtained, based on three kinds of molecular geometry, are very similar to each other. To simplify the discussion, only the results based on the optimized geometry will be considered hereafter.

The AO coefficients of the fluorine $2p_z$ orbitals of CF_3TCNQ are negligible (Figure 4, left, Table 5). In contrast to that, the fluorine $2p_z$ orbitals of

TABLE 5 Molecular Orbital Energy and Atomic Orbital (AO) Coefficients of the LUMOs of CF_3TCNQ: Only the $2p_z$ AO Coefficients for Nonhydrogen Atoms and those of 1 s Orbital for Hydrogen Atoms are Given

Geometry	CF_3TCNQ (I)	CF_3TCNQ (II)	Optimized
Energy (eV)	−3.1900	−3.3100	−3.1590
Atom C1	0.2839	−0.2781	−0.2916
C2	−0.3075	0.3058	0.3163
C3	−0.3168	0.3094	0.3203
C4	−0.2255	0.2215	0.2115
C5	0.2615	−0.2524	−0.2458
C6	0.2730	−0.2767	−0.2645
C7	0.0607	−0.0567	−0.0657
C8	0.4599	−0.4600	−0.4370
C9	0.0601	−0.0601	−0.0658
C10	−0.0528	0.0519	0.0540
C11	−0.4238	0.4318	0.3743
C12	−0.0493	0.0499	0.0500
C13	0.0198	−0.0197	−0.0245
N14	−0.1810	0.1786	0.1861
N15	−0.1790	0.1847	0.1864
N16	0.1602	−0.1662	−0.1574
N17	0.1626	−0.1725	−0.1592
F18	0.0114	−0.0130	−0.0022
F19	0.0174	−0.0180	−0.0253
F20	−0.0072	0.0083	0.0027
H2	−0.0050	0.0029	0.0064
H4	0.0038	0.0019	0.0009
H5	−0.0005	−0.0008	−0.0037

For the numbering scheme of the atoms, see Figure 3b.

F_2TCNQ conjugate well with the π-system of TCNQ moiety and show the AO coefficients of 0.10 and 0.13 in absolute values in the LUMO and HOMO, respectively (Figure 4, right). It should be noted that the C-F bonds of F_2TCNQ are antibonding, indicating that the frontier orbitals of the π-moiety are destabilized by the conjugation with the fluorine atoms from the point of the orbital interaction. This situation is similar to that of the theoretical explanation of the "perfluoro effect" in the photoelectron spectroscopy: ***the substitution of fluorine for hydrogen in a planar molecule has much larger stabilizing effect on the σ MOs than on the π MOs*** [18]. Accordingly, the direct substitution by fluorine of the hydrogen atom of TCNQ increases or decreases the acceptor strength by inductive or mesomeric effect, respectively.

The degree of conjugation between the electron-withdrawing substituent and the carbon atom to which the substituent is attached is different between these compounds. In F_2TCNQ both the fluorine and the

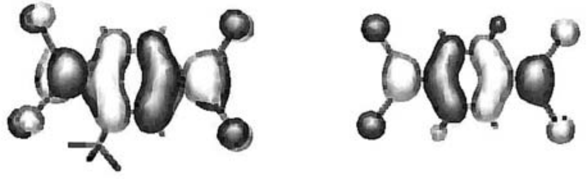

LUMO of CF_3TCNQ LUMO of F_2TCNQ

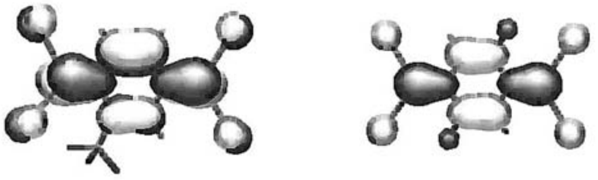

HOMO of CF_3TCNQ HOMO of F_2TCNQ

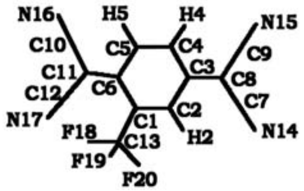

FIGURE 4 Schematic representation of the AO coefficients of MOs. Frontier orbitals of CF_3TCNQ (left) and F_2TCNQ (right) are compared. For CF_3TCNQ, see also Figure 3 and Table 5.

carbon atoms show significant $2p_z$ AO coefficients (>0.09) in 6 MOs out of 74. On the other hand, only 3 out of 83 MOs of CF_3TCNQ satisfy the same criterion; namely both the 2pz AO coefficients of C1 and C13 exceed 0.09 in absolute value. Furthermore, two of these show the bonding combination between C1 and C13. These results clearly indicate that the fluorine atoms and the π-system do not conjugate well in CF_3TCNQ, hence the strong electron affinity is ascribed to the inductive effect rather than the mesomeric one of the CF_3 group.

FORMATION OF SOLID CT COMPLEX OF CF_3TCNQ

A variety of aromatic hydrocarbons, aromatic amines and diamines, TTF derivatives, organic and inorganic cations, etc. afforded solid CT complexes of CF_3TCNQ. The high solubility of these CF_3TCNQ complexes in conventional organic solvents rendered the isolation of CT crystals rather difficult. This tendency stems from the highly soluble nature of the acceptor molecule, for example, 0.1 g/ml in MeCN and 0.02 g/ml in benzene. A variety of solid CT complexes concerned with the stoichiometry, structure, electric and magnetic properties, and optical property were prepared. For example, D:A being 1:1 (with alkali metals, TTF, TMTTF) and 1:2 (with 1,3,6,8-tetrakisdimethyaminopyrene) fully ionic insulators, 2:1 metals (with BEDO-TTF, EOET-TTF), 2:1 (with BEDT-TTF, BEDO-DBTTF) and 1:x ($x < 1$) (with BEDT-TTF, HMTTeF) highly conductive semiconductors and 1:1 neutral insulators (with pyrene, perylene) were obtained. Their crystal structures, and electrical, magnetic, and optical properties will be reported separately.

SUMMARY

In summary we have described the synthesis, physical properties and crystal structure of a TCNQ derivative with low symmetry, trifluoromethyl-TCNQ (CF_3TCNQ). CF_3TCNQ is very soluble in conventional organic solvents. It is a strong electron acceptor, comparable to 2,5-difluoro-TCNQ, and affords a variety of solid CT complexes. The dihydro-compound CF_3-H_2TCNQ is a strong Brönsted acid.

REFERENCES

[1] J. P. Ferraris, D. O. Cowan, V. V. Walatka, and J. H. Perlstein, *J. Am. Chem. Soc.*, **95**, 948–949 (1973).

[2] (a) T. Nakamura, G. Yunome, R. Azumi, M. Tanaka, H. Tachibana, M. Matsumoto, S. Horiuchi, H. Yamochi, and G. Saito, *J. Chem. Phys.*, **98**, 1882–1887 (1994).
(b) K. Ogasawara, T. Ishiguro, S. Horiuchi, H. Yamochi, and G. Saito, *Jpn. J. Appl. Phys.*, **35**, L571–L573 (1996).

[3] Y. Iwasa, N. Watanabe, T. Koda, and G. Saito, *Phys. Rev.*, **B47**, 2920–2923 (1993).

[4] S. Niwa, *Synth. Metals*, **18**, 665–670 (1987).

[5] (a) R. S. Potember, T. O. Poehler, D. O. Cowan, and A. N. Bloch, in *The Physics and Chemistry of Low Dimensional Solids*, ed. L. Alcacer (D. Reidel Pub. Co., Dordrecht, Holland, 1980, p. 419.
(b) Y. Iwasa, T. Koda, Y. Tokura, S. Koshihara, N. Iwasawa, and G. Saito, *Appl. Phys. Lett.*, **55**, 2111–2113 (1989).

[6] T. Goto, T. Kondoh, K. Egawa, and K. Kubodera, *J. Opt. Soc. Am. B*, **6**, 703–706 (1989).

[7] (a) G. J. Ashwell, E. J. C. Dawnay, A. P. Kuczynski, M. Szablewski, I. M. Sandy, M. R. Bryce, A. M. Grainger, and M. Hasan, *J. Chem. Soc. Faraday Trans.*, **86**, 1117–1121 (1990).
(b) M. Szablewski, P. R. Thomas, A. Thornton, D. Bloor, G. H. Cross, J. M. Cole, J. A. K. Howard, M. Malagoli, F. Meyers, J.-L. Bredas, W. Wenseleers, and E. Goovaerts, *J. Am. Chem. Soc.*, **119**, 3144–3154 (1997).

[8] (a) R. M. Metzger and C. A. Panetta, in *Lower-Dimensional Systems and Molecular Electronics*, eds. R. M. Metzger, P. Day, and G. Papavassiliou (Plenum, New York, 1990) p. 611.

(b) R. M. Metzger, B. Chen, H. Hophner, M. V. Lakshmikantham, D. Vuillaume, T. Kawai, X. Wu, H. Tachibana, T. V. Hughes, H. Sakurai, J. W. Baldwin, C. Hosch, M. P. Cava, L. Brehmer, and G. J. Ashwell, *J. Am. Chem. Soc.*, **119**, 10455–10466 (1997).

[9] H. Suzuki, A. Kondo, and T. Ogawa, *Chem. Lett.*, **411** (1985).

[10] M. Uno, K. Seto, M. Masuda, W. Ueda, and S. Takahashi, *Tetrahedron Lett.*, **26**, 1553–1556 (1985).

[11] (a) R. C. Wheland and E. L. Martin, *J. Org. Chem.*, **21**, 3101–3109 (1975).
(b) D. S. Acker and W. R. Hertler, *J. Am. Chem. Soc.*, **84**, 3370–3374 (1962).

[12] (a) C. G. Swain and E. C. Lupton, Jr., *J. Am. Chem. Soc.*, **90**, 4328–4337 (1968). Plots of the redox potentials vs. $\Sigma(\sigma_m+\sigma_p)/2$ (or $\Sigma\sigma_p$) for $(MeO)_2$TCNQ and $(EtO)_2$TCNQ deviate considerably from the line which has been experimentally observed for many other TCNQs. The best fit was obtained by using $\Sigma\sigma_p$ for $(MeO)_2$TCNQ and $(EtO)_2$TCNQ while $\Sigma(\sigma_m+\sigma_p)/2$ for other TCNQs in this work.
(b) R. C. Wheland and J. L. Gillson, *J. Am. Chem. Soc.*, **98**, 3916–3925 (1976).
(c) L. Bucsis and H. Kiesele, *Acta Chim.* (*Budapest*), **93**, 141–148 (1997).
(d) G. Saito and J. P. Ferraris, *J. C. S., Chem. Commun.*, **1027** (1979).

[13] E. C. M. Chen and W. E. Wentworth, *Mol. Cryst. Liq. Cryst.*, **171**, 271–285 (1989).

[14] T. Senga, K. Kamoshida, L. A. Kushch, G. Saito, T. Inamoto, and I. Ono, *Mol. Cryst. Liq. Cryst.*, **296**, 97–143 (1997).

[15] G. Saito, T. Teramoto, A. Otsuka, Y. Sugita, T. Ban, M. Kusunoki, and K. Sakaguchi, *Synth. Metals*, **64**, 359–368 (1994).

[16] (a) T. Akutagawa and G. Saito, *Bull. Chem. Soc. Jpn.*, **68**, 1753–1773 (1995).
(b) T. Akutagawa, G. Saito, M. Kusunoki, and K. Sakaguchi, *Bull. Chem. Soc. Jpn.*, **69**, 2487–2511 (1996).

[17] T. J. Emge, M. Maxfield, D. O. Cowan, and T. J. Kistenmacher, *Mol. Cryst. Liq. Cryst.*, **65**, 161–178 (1981).

[18] C. R. Brudndle, M. B. Robin, N. A. Kuebler, and H. Basch, *J. Am. Chem. Soc.*, **94**, 1451–1465 (1972).